Technology and Health Care 11 (2003) 425–441
IOS Press

A system for the acquisition of reproducible digital skin lesions images

Ilias Maglogiannis[a,*] and Dimitrios I. Kosmopoulos[b]
[a]*University of Aegean, Department of Information and Communication Systems Engineering, 83200 Karlovasi, Greece*
[b]*National Technical University of Athens, School of Electrical and Computer Engineering, 15773 Athens, Greece*

Received 27 March 2003
Revised 30 June 2003

Abstract. A major issue concerning the design and implementation of an image acquisition system for skin lesions is its ability to capture reproducible images. The reproducibility is considered essential for image analysis and for the comparison of sequential images during follow-up studies. This paper describes a prototype image acquisition system that includes a standardized illumination and capturing geometry with polarizing filters and a series of software corrections: Calibration to Black, White and Color for color constancy, Internal camera Parameters adjustment and Pose extraction for stereo vision, Shading correction and Noise Filtering for color quality. The validity of the calibration procedure and the images' reproducibility were tested by capturing sample images in three different lighting conditions: dark, medium and intense lighting. For each case the average values of the three color planes RGB and their standard deviations were calculated; the measured error differences ranged between 0.7 and 12.9 (in the 0–255 scale). Preliminary experiments for stereo measurements provided repeatability of about 0.3 mm. The above results demonstrate the reproducibility of the captured images at a satisfactory level. The developed prototype was also evaluated clinically, for its ability to support the construction of knowledge-based decision systems and for telemedicine, thus to support telemedical sessions in dermatology.

Keywords: Skin lesion inspection, reproducible images, camera calibration, color constancy, image analysis, telemedicine

1. Introduction

So far, dermatologists have based the diagnosis of skin lesions on the visual assessment of pathological skin and the evaluation of macroscopic features. Therefore, the diagnosis has been highly dependent on the observer's experience and on his or her visual acuity. However, the human vision lacks accuracy, reproducibility and quantification in gathering information from an image and systems that are able to evaluate images in an objective manner are obviously needed.

Recently there has been a significant increase in the level of interest in image morphology, full-color image processing, image recognition, and knowledge-based image analysis systems for skin lesions. The quantification of tissue lesion features in digital images has been proven to be of essential importance in clinical practice. Several tissue lesions can be identified through measurable features that are identified

*Address for correspondence: Dr. I. Maglogiannis, University of the Aegean, Department of Information and Communication Systems Engineering, 83200 Karlovasi, Greece. Tel.: +30 2273 82239; Fax: +30 2273 82009; E-mail: imaglo@aegean.gr.

in digital images. Such features are related to lesion geometry or its color properties. If selected properly the features can give objective indications on the lesion status; even small differences in the lesion features may provide reliable indications about the patient's reaction to therapeutic measures; therefore accuracy in the measurements of the related features is highly desired [7,8,12,17,20,21,25,26]. The more accurate are the measurements, the faster and more flexible may be the adaptation of the therapeutic procedures in the individual patient needs.

The first step in such an image analysis system intended for evaluation of skin lesions involves the acquisition of the tissue digital image. Probably the most important problem, which has to be resolved concerning the design and implementation of the acquisition system, is its ability to capture reliable and reproducible images. The reproducibility is considered essential for image analysis classification and for the comparison of sequential images during follow-up studies. However, the acquisition of reproducible images remains challenging due to equipment and environmental constraints such as image resolution, image noise, color representation, illumination, skin reflectivity and pose uncertainty.

This work presents a new methodology for generating sets of reproducible color lesion images with minimized reflections and shading. In the next section we describe the aforementioned constraints and in Section 3 we present a complete system for acquisition and processing of reproducible images. In Sections 4 and 5 we describe the camera calibration and the processing that is performed online. In Section 6 we provide the image capturing standardized procedure and the initial experimental results. Section 7 discusses the potential use of the system for telemedicine and finally Section 8 concludes the paper.

2. Image acquisition limitations and related background

In this section we present the equipment and environmental constraints that adversely affect the reproducibility of images of a skin lesion. These can be summarized to:

(a) low image resolution due to equipment limitations;
(b) misalignment of frames acquired with interlaced cameras;
(c) shading and noise due to sensor limitations or other particles on skin, e.g., hairs;
(d) color quality and constancy;
(e) variable environment illumination;
(f) reflections due to skin nature and illumination constraints;
(g) pose uncertainty due to target movement.

The use of commercially available photographic cameras is quite common in skin lesion inspection systems, particularly for telemedicine purposes [15]. However, the poor resolution in very small skin lesions (i.e. lesions with diameter of 0.5 cm or less) and the variable illumination conditions are not easily handled and thus these devices, have been proven insufficient for capturing skin lesions with high requirements in resolution and color measurement [21]. The new models with higher resolution that are expected in the near future, are anticipated to solve the first problem. The second problem though, considered necessary for the reproducibility of the images will probably remain unsolved, as it requires real time, automated color calibration of the camera. Color calibration refers to the adjustments and corrections that are necessary, so that the camera works within its dynamic range and measures always the same color regardless of illumination. The calibration procedure is a rather complex difficult and very sensitive task, which is not expected to be incorporated soon as a full function in commercial models. The problem can be solved to some extend by using video cameras that are parametrizable online and can be easily controlled through software. Zoom lenses and subpixel image processing can be used for increasing the measurement accuracy.

The problem of frame misalignment due to the interlaced acquisition is quite common and may have serious negative effects on the image quality. Even slight target movements relative to the camera can distort the image (e.g., [6]). It has been treated in the past through separate processing of even and odd frames, which could lead to loss of information. The use of progressive-scan non-interlaced cameras solves this problem.

The image noise is mainly attributed to the finite spatial resolution of the CCD chips, which filters out the high spatial frequencies (sharp edges). Moreover, the limitations of the image acquisition hardware (sensor elements, digitizer) cause the pixel values to fluctuate within some limits (color values). Cross-talking between neighboring pixels is also a factor that contributes in noise. The skin lesion color is adversely affected by noise thus leading to unreliable results concerning the lesion status. Particles of variable geometric characteristics on the skin such as hairs, dust etc. cause additional problems to the reproducibility of the acquired images. Noise can be eliminated through appropriate filtering, e.g., morphological filtering to preserve edge information [5] or median filtering to assist color identification [26]. Furthermore, all imaging systems produce shading. By this we mean that if the physical input image $a(x, y) = \mathrm{constant}$, then the digital image will not be constant. The source of the shading might be the result of a variable gain and offset from pixel to pixel. The method by which images are produced – the objects in real space, the illumination, and the camera – frequently leads to situations where the image exhibits significant shading across the field-of-view. In some cases the image might be bright in the center and decrease in brightness as one goes to the edge of the field-of-view. In other cases the image might be darker on the left side and lighter on the right side. The shading might be caused by non-uniform illumination, non-uniform camera sensitivity, or even dirt and dust on glass (lens) surfaces. Shading effect is extremely undesirable in image analysis systems, as it affects the color accuracy of the CCD camera. Eliminating it is frequently necessary for ensuring the reproducibility of the skin digital images.

Another issue of concern is the quality and the consistency of color information. The acquisition hardware may produce images with colors that differ significantly from the colors perceived by humans, thus leading to low color reproduction quality. A related problem is the acquisition of consistent color images (color constancy), which remains a challenging task especially when diverse acquisition hardware is used, mainly due to the non-uniform sensor responses to the same illumination.

The scene illumination is probably the most influential factor on lesion inspection. Non – constant scene illumination may lead to totally different and thus non-reproducible images. Therefore, engineering of the environment is applied, to enforce constant illumination conditions. Moreover, a major problem in digital skin image acquisition involves the reflections of the incident light. The human skin, because of its irregular surface, scatters incident light in irregular directions, burying diagnostic information. A technique introduced in the past has involved the use of glass, positioned between the camera and the skin tissue so that the breaking surface is flat and with appropriate lighting geometry it is possible to avoid the reflections. This arrangement allows the isolation of the region of interest from the environment and can ensure reproducibility of the lighting conditions. However, the biggest drawback of the specific arrangement is that the pressure impressed on the skin tissue is not measurable or reproducible and stimulates local hematoma, which changes the color and the morphology of the skin [1].

The problem of measuring features on skin lesions using single images is – apart from color extraction – a problem of inferring 3D structure and distance from a two-dimensional image. The shape of the inspected area is not known in advance and therefore no known patterns of the target can be used to extract

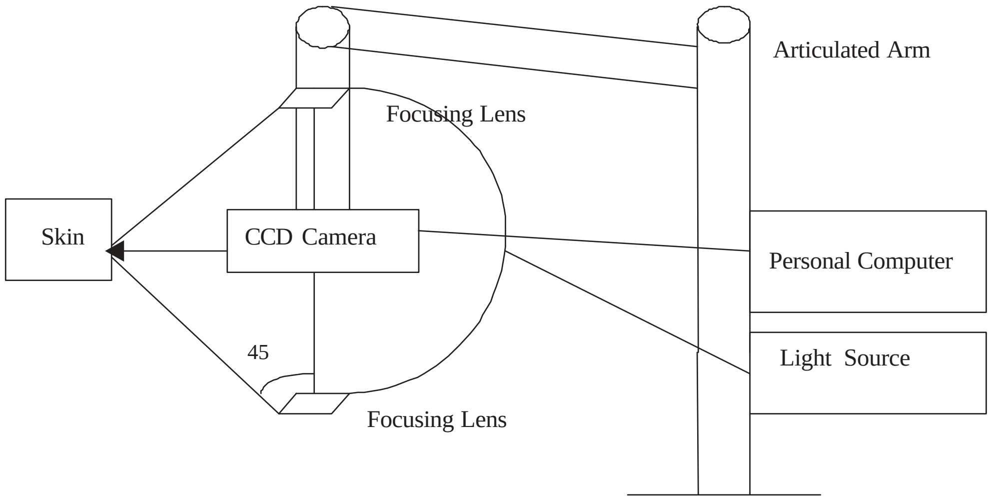

Fig. 1. The lighting geometry of the image acquisition system consists of a color video camera, two focusing lenses (mounted on an articulated arm) that face the target at an angle of 45 degrees, a light source that sends light to the lenses through fiber optics and a personal computer for image processing.

pose information. A simple solution that provides estimation of the lesion dimensions is to assume that the whole skin area of interest lies on the same plane and to attach known artificial patterns (e.g., a ruler, sets of circles, rectangles etc.) on it, in a way that they do not obstruct the measurements [28]. Through these patterns the pose of the skin plane and consequently the relative distances can be extracted. The method is simple, but it can track reliably only the gross differences in follow-up studies, mainly due to the fact that the attached patterns do not actually lie on the same plane with the target. The skin is not solid and therefore slight patient movements may displace the attached patterns causing poor accuracy in dimension calculation. The method also depends on how accurately we know the dimensions of the artificial pattern. Bigger and more complex patterns may yield better results but sometimes the attachment of such patterns is impossible or undesired due to the skin nature in the target area. Furthermore, artificial patterns are normally placed near the edge of the image, where the distortion due to the lens is higher; this deteriorates the accuracy.

In the next section we present a new system for digital image acquisition that handles the problems (a)-(c), (e)-(f) and color constancy in (d). Additionally we show how we can solve (g) by endowing this system with stereo-vision capabilities.

3. Image acquisition installation

In this section we present a digital image acquisition system that is able to handle the common problems of low resolution, frame misalignment, shading and noise, color constancy, target illumination, skin reflections and pose uncertainty. The system is displayed in Fig. 1 and it includes two light sources (lamps) and a color camera, which are mounted on an articulated arm, and a processing PC.

The lamp's light is transmitted and delivered onto the surface at an angle of approximately 45° and the reflected light is collected at about 0° to the surface normal. This illumination and capturing geometry is internationally established for color measurements, because it reduces shadows and reflections [29]. The system provides the possibility to define regions of interest manually and therefore the ability to

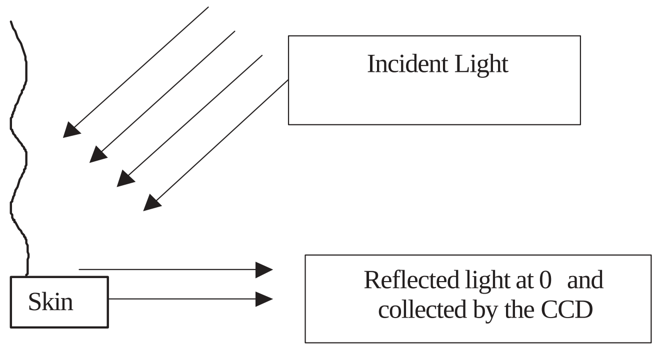

Fig. 2. Partial Reflection at 0° due to the curved surface of the skin.

optimize the illumination for that limited region. Thus systematic errors due to non-homogeneous light, which are common to chromatometers are avoided.

Regarding light source, in the past incandescent lamps had a significant advantage over fluorescent lamps in the area of color rendering; however, newer fluorescent lamps have excellent color rendering ability. To optimize color rendering ability, lamp temperature should be at least within the 2900–3300 Kelvin range, with a Color Rendering Index (degree of ability to produce light output optimal for true color rendering) of 85 or higher [11,27]. For our prototype we have sought to achieve image reproducibility but also to keep the cost low by using off-the-shelf components. Therefore we have used halogen illumination (3300 Kelvin), which proved cost-effective. Using Xenon or Metal Halide lamps, which have color temperature much closer to the daylight (e.g., 5300–6500 Kelvin), would improve color rendering, which is especially useful for image capturing applications, but would also rise significantly the illumination cost (by a factor 10 or more).

Although the above geometry effaces most of lighting reflections, it is very difficult to create uniform illumination at an angle over 45° over the entire field of view and over curved surfaces as the human skin. This situation is depicted in Fig. 2, where a partial reflection at 0° exists, due to the curved surface of the skin. This was observed also through experimenting with the implemented systems as displayed in Fig. 4a. Our system eliminates the remaining reflections through additional polarizing filters. The functionality of the filters can be explained if we consider light as an electromagnetic wave, oscillating in an arbitrary direction perpendicular to its motion direction. A polaroid filter transmits only the component of the oscillation that is directed in the polarizing direction of the filter. So only the waves that are oscillating in the polarizing direction can pass unattenuated. All other waves will attenuate according to the formula:

$$\mathrm{Amplitude\ after\ polarizing} = \mathrm{Amplitude\ before\ polarizing} * \cos(\mathrm{theta}) \tag{1}$$

where $theta$ is the angle between the oscillating direction of the wave and the polarizing direction of the filter. Thus we may minimize reflections by positioning two polarizing filters in front of the light source and the camera and by adjusting their polarizing directions vertically. The effect of the polarizing filters is demonstrated in Fig. 4. In Fig. 4a $theta = 0$ and in Fig. 4b $theta = 90$ degrees.

In our system we use a CCD camera. An alternative selection could be the newly introduced CMOS–based camera. CMOS cameras offer onboard signal processing functionality at a fraction of the cost of CCDs and have much better onboard programmability for more efficient read-outs and easier integration with “off-the-shelf” digital signal processors; however, the CMOS imaging array usually suffers from limited dynamic range when compared to CCDs and will saturate in over- or under-exposed scenes [3,

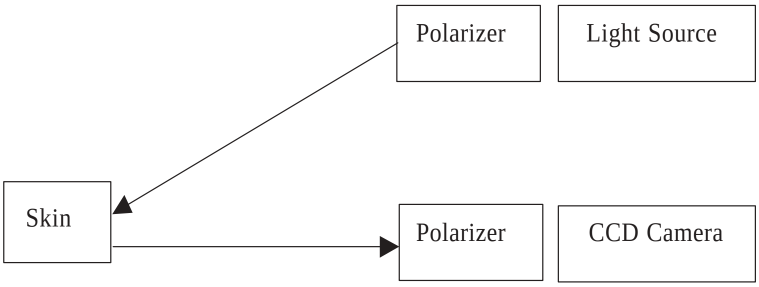

Fig. 3. A polarizing filter transmits only the component of the oscillation that is directed in the polarizing direction of the filter. The angle between the directions of the two polarizers is set to 90 degrees to eliminate light reflections.

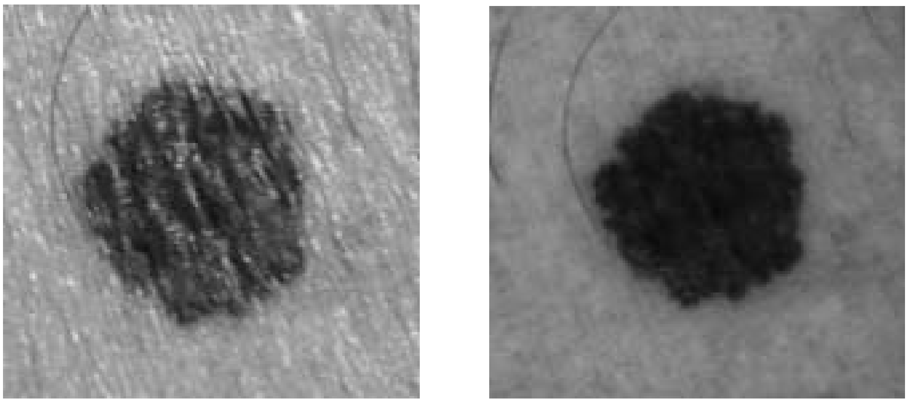

a b

Fig. 4. Skin lesion image acquired with polarizing filters (a) in parallel relative position and (b) in vertical relative position. In the second case the reflections are significantly reduced.

35]. The remedy of this deficiency, may lead to replacement of the CCD sensors in systems such as ours by the CMOS sensors.

Summarizing, the implemented image acquisition system as it is illustrated in Fig. 1 consists of:

– A 3-chip CCD color video digital video camera (Panasonic GP-US502) with resolution 811(H) $\times$ 508(V) pixels in visible spectra and an RGB output. It comes with a built-in digital signal processing (DSP) circuit for noise reduction and better operability.
– A 150-W, 21-V quartz halogen lamp, with color temperature of 3300 K, which delivers a relatively smooth spectrum without many spikes.
– A Personal Computer
– Circular polarizing filters in front of the CCD receiver and the light focusing lens.

The system that is presented so far is able to measure lesions in 2D images. This provides lower accuracy in dimension measurements as explained in Section 2. This problem can be overcome through stereo-vision. By using a pair of calibrated cameras the geometrical features can be measured with high accuracy. In this case any artificial pattern on the target becomes redundant because the lesion pose can be estimated by measuring directly the target.

The system is extended by adding one more camera and keeping almost the same illumination configuration. The cameras are synchronized to ensure simultaneous image grabbing. The cameras are placed

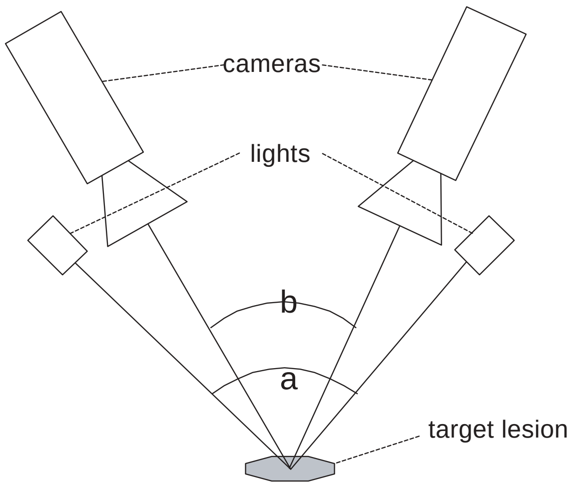

Fig. 5. The stereo installation consisting of two cameras with relative angle $b \approx 15 - 20$ degrees and two lights with relative angle $a = 45$ degrees.

with their x-axes on the same plane and their y-axes in parallel; in order to ensure uniform measurements in all dimensions their z-axes have to intersect at ideally $b = 90$ degrees [19]; on the other hand, to avoid reflections as mentioned previously and to assist the stereo matching the angle b has to be small (ideally zero). Through experimentation we have found that the configuration that provides low reflections, good matching and acceptable accuracy has an angle b of about 15–20 degrees, depending on the target's curvature and shape.

4. Camera calibration

Before the system is able to acquire images the cameras have to be calibrated. Calibration is performed offline and it regards (1) color and (2) camera pose and camera internal parameters. The calibration regarding each of the above aspects will be examined in the following subsections.

4.1. Calibration to color

For input devices such as cameras or scanners calibration to color means establishing the relationship between an original color and the output image. For output devices such as displays or printers this means establishing the relationship between the signals sent to the device and the produced color (emitted light or ink on paper). The calibration if executed properly may ensure high color quality and high reproducibility.

The pixel values provided by the sensor depend on the sensor response, the illumination and the reflectivity of the viewed object. To perform acquisition of reproducible color images we have to achieve color constancy independently of the used camera or the illumination variances. The calibration of our system is performed in two steps: (a) calibration to black and white and (b) calibration with regard to the Macbeth color chart for color constancy.

The calibration to black and white includes comparing camera response to black and white standards with their known lightness and appropriate modification of intensity output values. This procedure requires the calculation of two images – *BLACK* and *WHITE* (three-dimensional arrays of pixel values).

The *BLACK* image is calculated as the average of a set of frames that are acquired after covering the lens (we have averaged thirty frames). It corresponds to an image matrix, which should have ideally zero values for all pixels. The following equation holds:

$$\mathrm{BLACK}\ [c, m, n] = \mathrm{offset}[c, m, n]. \tag{2}$$

where c is the color plane (red, green, blue) m, n are the pixel x, y coordinates and *offset* is the CCD error for zero input. The *WHITE* image is calculated as the average of a frames set capturing the perfect diffuser $BaSO_4$ (we have averaged thirty frames). *WHITE* image corresponds to an image matrix, which should give ideally a value of 255 for all pixels. Supposing that $I_w[c, m, n]$ is the ideal image we have:

$$\mathrm{WHITE}[c, m, n] = \mathrm{gain}[c, m, n] \cdot I_w[c, m, n] + \mathrm{offset}[c, m, n]. \tag{3}$$

If $a[c, m, n]$ is the captured image, then the correction becomes:

$$I[c, m, n] = (a[c, m, n] - \mathrm{BLACK}[c, m, n]) \cdot I_w[c, m, n]/(\mathrm{WHITE}[c, m, n] - \mathrm{BLACK}[c, m, n]) \tag{4}$$

During the black and white calibration it should be ensured that the CCD is functioning in its dynamic range and is not saturated. This is done by adjusting the iris electronically until one of the three RGB channels is 255, while the other two are close but below 255. Black and White calibration is then performed to each of the RGB channels separately.

The possible problem of the image being bright in the center and darker as one goes to the edge of the field-of-view (shading) is handled through appropriate shading correction. Shading correction is performed by division of an image with all pixels having R=G=B=255 by the white reference image (previously calculated) and then multiplying a captured image with the look-up table generated by the division.

The responses of the cameras are generally non-linear in a non-uniform manner. Therefore, apart from calibration to black/white and shading correction, to achieve constancy for the intermediate colors we have to perform colorimetric calibration. The primary methods reported for colorimetric calibration include among others, 3D look-up tables (e.g., [9]), reflectance calculation from characteristic vector analysis (e.g., [13]), least squares polynomials (e.g., [4]), neural networks (e.g., [10]), and set theoretic approaches (e.g., [32]). However, these approaches require procedures and additional equipment that are too complicated for a system that is destined to be used in a hospital environment by rather inexperienced personnel.

The main requirement of our system is the acquisition of uniform colors independently of the external illumination or the response of the acquisition system and it is fulfilled by a quite simple but effective approach: we use the Macbeth Color Checker to map the responses of the present system to the responses of a reference system and we construct a look-up table. The Macbeth Color Checker [33] is a checkerboard array of 18 colored and 6 neutral charts, which reflect light in the visible spectrum.

For the reference measurements we seek to implement the directives described in Section 3 trying to minimize the influence of external illumination. For our calibration procedure we acquired images of the Macbeth Color Checker. For each of its color charts we acquired 30 images at various moments, taking care that the charts were located near the image center, to minimize the undesired geometric effects of the acquisition system. To extract the values we have averaged the pixel values of image windows of size 20×20 for all the acquired frames. The resulting RGB values formed the reference values for the eighteen color charts. The procedure is illustrated in Fig. 6a.

Each time that the acquisition system or the illumination changes, a similar procedure has to be repeated. The resulting average RGB values for the charts are mapped to the reference values and from

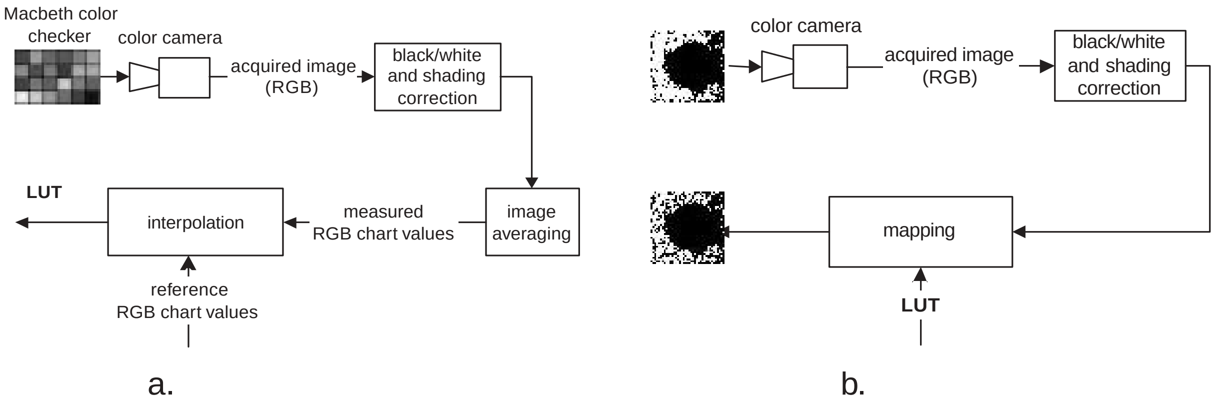

Fig. 6. (a) The color calibration procedure: images of the Macbeth Color Checker are acquired, for each image black/white and shading correction is applied, the images are averaged, the measured are combined with the reference values to construct a look-up table. (b) The acquisition of reproducible color images: the acquired image is corrected with regard to black/white and shading and from the look-up table the new image is calculated.

these mappings a look-up table is constructed for each channel. The intermediate values are interpolated using cubic polynomials. The procedure is illustrated in Fig. 6b.

The main advantage of this approach is that it provides acceptable accuracy while we do not need prior knowledge of the Macbeth Color Checker charts' reflectivity, of the illumination spectrum and of the camera response to it. Therefore no additional equipment (e.g., spectrophotometers, colorimeters) is required and a system can be calibrated in a relatively easy manner.

4.2. Calibration to pose and camera internal parameters

The calibration for the external and internal camera parameters is required to perform stereo triangulation. The former define the cameras' pose (rotation matrix **R** and translation vector **T** from world to camera coordinates) and the latter define how incident light is projected onto the CCD plane. All parameters are obtained through the calibration procedure. From the methods that appear in the related literature we have used the one introduced by Tsai and Lenz [14,24] due to its versatility and high accuracy[1] compared to other methods [22]. The calculated internal parameters are

- the effective focal length of the pinhole camera;
- the first order radial lens distortion coefficient;
- the coordinates of the center of the radial lens distortion;
- a scale factor that accounts for uncertainties due to frame grabber horizontal scanline resampling.

As a calibration pattern we have used a metal plate with an array of 8×8 black circles that are etched with accuracy better than 0.05 mm (Fig. 7). Their radius is 2.5 mm and the centers of neighboring circles have a distance of 10 mm; it covers the image area, where the target is expected to appear. The external camera parameters are set with respect to the central circle of the plate. The calibration is performed separately for each color plane.

[1]The code that we used was adapted from the freeware version provided by Carnegie Mellon University.

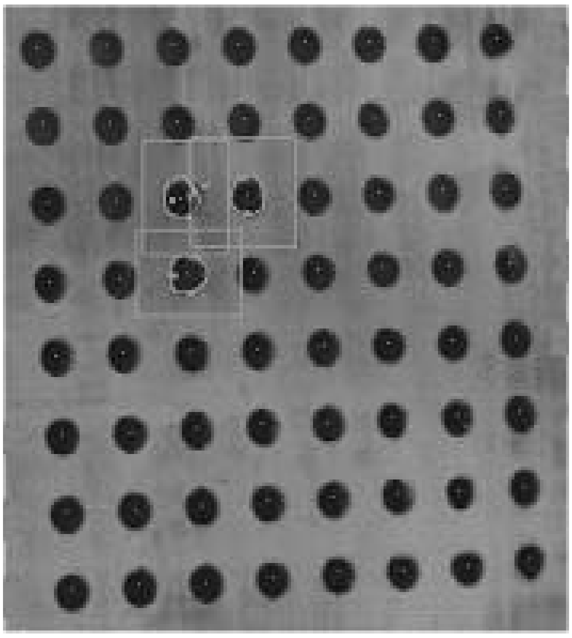

Fig. 7. The calibration pattern is metal plate with an etched array of 8×8 dark circles on a light background.

5. Online processing

The image acquisition system described in this paper, is the first step in the development of a complete image analysis system for dermatological images. An image analysis system requires the extraction of border and color-based features, which are used for the evaluation and the classification of the digital images containing the skin lesions. The feature extraction is performed by measurements on the pixels that represent the skin lesion. During the clinical trial of the developed system we tried the evaluation of some dermatological images and particularly the recognition of two set of images containing malignant melanoma versus dysplastic nevus. Although these lesions have common appearance, the first is fatal cancer while the second is a rather harmless disease. A frequently encountered problem is the misdiagnosis of melanoma as dysplastic nevus by non expert dermatologists.

The border-based features computed were Greatest Diameter, Area, Border Irregularity, Thinness Ratio, and Border Asymmetry. Border Asymmetry was computed as the percent of non-overlapping area after a hypothetical folding of the border around the greatest diameter, while Irregularity and Thinness Ratio were calculated by the following equations:

$$\mathrm{Irregularity} = \mathrm{Perimeter}/\mathrm{Area} \tag{5}$$

$$\mathrm{Thinness\ Ratio} = 4\pi \frac{\mathrm{Area}}{(\mathrm{Perimeter})^2} \tag{6}$$

The second feature category involves the values of the pixels that are located inside the border and thus correspond to the skin lesion. The color features were based on measurements on RGB color planes or other color planes such as HIS (Hue, Intensity, Saturation), HSV (Hue, Saturation, Value), HLS (Hue, Lightness, Saturation) and CMY (Cyan, Magenta, Yellow). Color variation was also calculated by measuring standard deviations of the RGB channels and chromatic differences inside the border. For the first category of features, which correspond to the physical dimensions of the lesion, 2-D or 3-D vision (for higher accuracy) may be used, while for the color based features color calibration is required.

To assist color identification we perform Median Filtering in a preprocessing stage. It is used for noise reduction due to hair, scales and light reflections. This procedure ends in blurring the image, which visually seems a poorer result but on the other hand assists the analysis procedure, as it removes noise.

During the stereo measurements we seek to calculate geometrical dimensions of the skin lesions using the original images (without applying Median Filtering). The measurements are performed indirectly through measuring the 3D position of some key points. Such points may belong to the contour, or may be computed indirectly and express some lesion properties (e.g., points that define the big and small axes of ellipsoids). Provided that the projections of the same point can be recognized in the image of both cameras, the 3D point can be computed through stereo triangulation (described in the related literature e.g., in [23]). By calculating the 3D reconstruction of a set of contour points – e.g., the lesion contour – we obtain the dimensions of interest only through 3-D vector subtractions.

The main issue faced by stereoscopic systems is the correspondence problem. Given the image point $\mathbf{p}_1$ corresponding to a 3D point $\mathbf{P}$ how can we find the projection $\mathbf{p}_2$ of the same point on the other camera? The problem is simplified by the fact that the $\mathbf{p}_2$ lies on the epipolar line, which is given by:

$$\mathbf{l} = \mathbf{R} \cdot \mathbf{S} \cdot \mathbf{p}_1 \tag{7}$$

where

$$\mathbf{S} = \begin{bmatrix} 0 & -T_z & T_y \\ T_z & 0 & -T_x \\ -T_y & T_x & 0 \end{bmatrix} \tag{8}$$

and (**T** is the translation from camera 1 to camera 2 and **R** is the corresponding rotation matrix. Both **R**, **T** are known from calibration (described in Section 4). A correlation-based metric between the $\mathbf{p}_1$ and the points of **l** may give the corresponding point. If we seek to match points that belong to the lesion contour we may apply the metric only around the contour points that intersect with the epipolar line to limit complexity; the contour is extracted in previous processing steps.

The processing steps that were described in this section are depicted in Fig. 8.

6. Measurement procedure and experimental results

The described image acquisition system was installed at the outpatient's department of Plastic Surgery and Dermatology in the "General Hospital of Athens G. Gennimatas". The standardization of the image acquisition procedure was ensured through a protocol, which was applied for each patient by the medical staff. The system operator was trained to control the basic functions of the camera (i.e. ON/OFF, auto/manual focus, zoom, iris shut) electronically with software installed in the PC, where the images were stored. The specific tasks included in the image acquisition protocol are the following:

1. Start the PC and run the software for camera controls and calibration.
2. Turn on the light source.
3. Place the tablet of the perfect diffuser ($BaSO_4$) in front of the CCD and at a distance of 30 cm (with its normal vector parallel to z-axis of the camera).

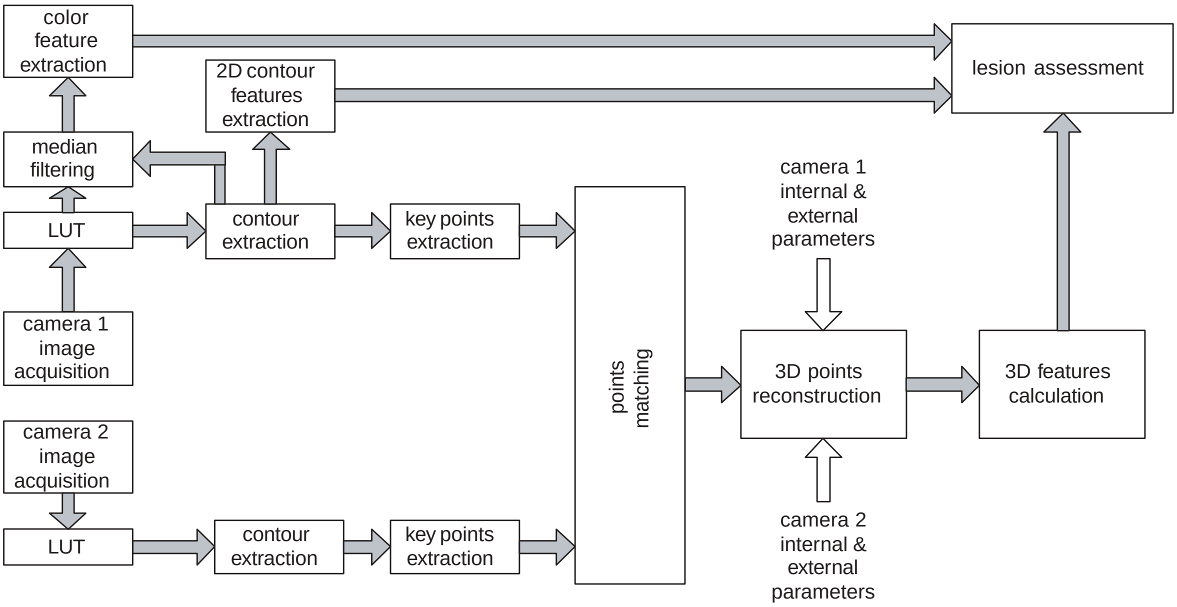

Fig. 8. The system as a whole. The 2D and 3D features along with the color features are used for assessment of the skin lesion images at a higher level. The processing is similar for the images of both cameras, however this is not depicted here for simplicity.

4. Adjust the iris electronically until one of the three RGB channels is 255, while the other two are close but below 255 (this ensures that the CCD is functioning in its dynamic range and is not saturated).
5. Cover the CCD sensor.
6. Perform calibration to black through the software.
7. Place again the tablet of the perfect diffuser (BaSO4) at the pose of step 3.
8. Perform calibration to white through the software.
9. Place the MacBeth color chart in front the camera at a distance of 40-50cm (with its normal vector parallel to z-axis of the camera). The captured charts have to be near the image center.
10. Perform colorimetric calibration.
11. Place camera opposite to the target with the skin lesion at a distance of 30-60 cm.
12. Adjust the polarizing filters to eliminate reflections.
13. Capture the image and store it into the database with the demographic data.

Steps 1 to 10 are followed only once by trained personnel. The steps 11–13 are trivial and can be performed easily by medical staff.

In order to assess the validity of the calibration procedure and the ability of the implemented image acquisition system to produce reproducible images we captured sample images in 3 different lighting conditions: dark, medium and intense lighting. Apparently the above setup protocol was applied each time the environmental lighting had changed.

For each case we captured and segmented repeatedly the same skin lesion and we calculated the average values of the three-color planes RGB and their standard deviation. The measured error differences ranged between 0.7 and 12.9 (in the 0–255 scale) for the average RGB values and 1.8 and 17.3 for their standard deviation. The corresponding mean errors were 7.6 and 12.3 or 7.6/255=2.98% and 11.5/255=4.51%.

Table 1
The measured error differences in RGB color plane between the 3 different lighting conditions

Type	Measured differences	
	Absolute (in the 0–255 scale)	Percentage (%)
Maximum difference for mean value	12.9	5.01
Maximum difference for standard deviation	17.3	6.78
Mean difference for mean value	7.6	2.98
Mean difference for standard deviation	11.5	4.51

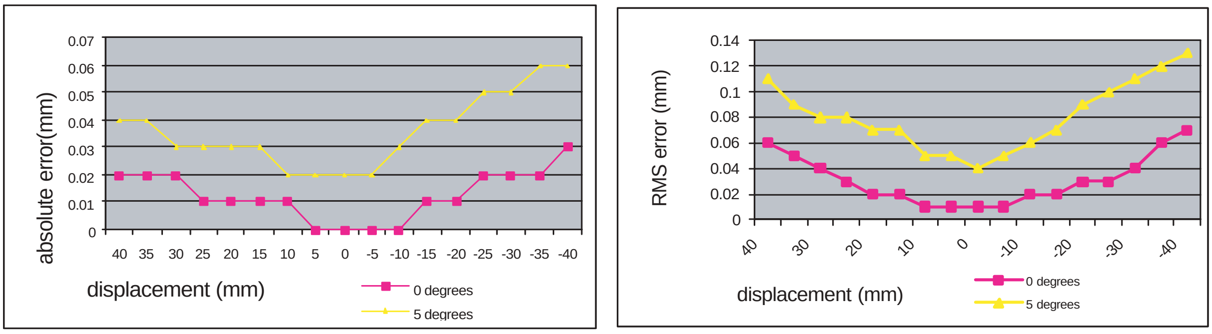

Fig. 9. Measurement of (a) the mean and (b) the RMS error for plate displacement of -40 to 40 mm and rotation of 0 and 5 degrees.

The above measurements concern only the color features of the captured images and they are summarized in Table 1.

Experimental results demonstrate the reproducibility of the captured images at a satisfying level. The remaining aberration is electronic noise caused by the CCD. A typical technique to eliminate this kind of noise, which is stochastic with zero mean value, is averaging sequential captured images of the same object. Unfortunately in our case the minor movements of the patient during the image acquisition prevent us from using this technique.

In the case of stereo measurements between the aforementioned steps 10 and 11 the following steps are additionally performed (only once by skilled personnel):

10a. Place calibration plate on nominal target position with its plane parallel to the plane that is approximately defined by the target lesion.
10b. Calibrate both cameras.

The presented stereo system has been tested so far extensively on synthetic features. We measured the distance between two coplanar points (nominal distance 10 mm) on a metal plate vertical to the symmetry axis of the installation presented in Fig. 5. The points were defined as the centers of two circles. We displaced the plate from -40 to 40 mm and rotated it 5 degrees with respect to the nominal pose to examine the effect of displacing the target lesion. The displacement is usually much smaller in actual situations ($\sim$5mm and 2–3 degrees). The rotation affects adversely the measurements but accuracy remains satisfactory for the application purposes. The fact that we measure relative distances and not absolute poses eliminates the systematic error. However, the measurement is adversely affected when displacing the target from the nominal pose, as revealed by the experiment, mainly because the camera parameters were locally optimized for the volume around that pose.

The system has been tested so far on real image pairs with promising results. The repeatability of the measurements for target displacement of a few mm and a few degrees from the nominal position was

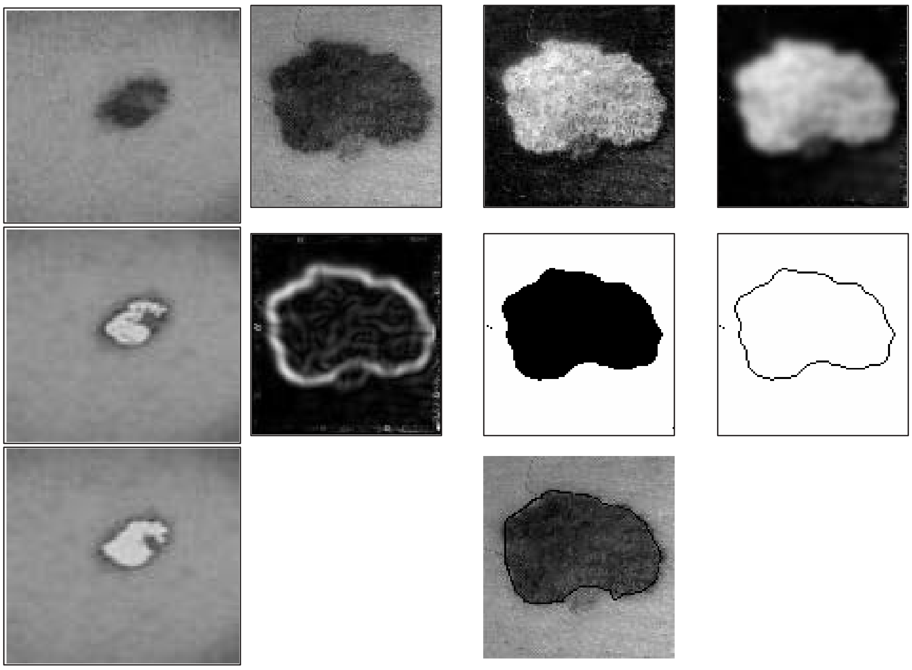

Fig. 10. Image segmentation of two skin lesions captured by the described system. Lesion on the left corresponds to dysplastic nevus and segmentation is performed through a Region Growing Technique. Lesion on the right corresponds to malignant melanoma and segmentation is performed through an Edge Detection Technique.

usually better than 0.3 mm (the "key points" in one camera were supposed to be known). Additional error is introduced by the additional image noise (due to reflections or the particles on skin) and by the point correspondence calculation.

In what concerns the lesion assessment based on the extracted features, we used linear discriminant analysis and a neural network model for image classification. Both the statistical method of discriminant analysis and the application of artificial neural networks led to high percentages of correct allocation of cases to their groups of origin, which proves the efficiency of the image capturing procedure. More specifically the discriminant analysis classified correctly 96.2% of cases (91% of melanoma and 100% of dysplastic nevus), while the neural networks models also performed very well. Using four principal components as input, the success rate achieved was 100%. This was reduced to 84.6% correct classification (82% of melanoma and 87% of dysplastic nevus) using only the first two principal components. Using Greatest Diameter and Thinness Ratio for input – that is, the two significant predictors identified above – gave 96.2% correct classification, exactly as in the discriminant analysis. Both methods, discriminant analysis and the neural network, misclassified the same cases of malignant melanoma as dysplastic nevus [18]. Figure 10 depicts two examples of images captured by the system and the initial processing for segmenting the skin lesion.

All the images captured by the system were stored in a database specially developed for this purpose along with other demographic and clinical data. This requirement was made by the medical personnel in order to correlate the occurrence of skin diseases with statistical parameters such as the patient's phototype, origin, profession, the UVE exposure, the co-existence of other diseases, the age of appearance etc.

7. The use of the system for telemedicine

The original scope of the designed system is image analysis and lession evaluation. However the application of telemedicine in dermatology is considered a quite important issue, since many studies (e.g., [30,31]) have proved that the general doctors are unable to diagnose successfully the common dermatological diseases. Therefore in our study we attempted to use the developed system for telemedical purposes as well.

Telemedical evaluations in dermatology are based mainly on the visual assessment of the transferred digital images of skin lesions. Under this perspective the reliability and reproducibility of the skin lesions colour in the captured images is essential for a correct distant diagnosis of a cutaneous disease. In digital image analysis we only deal with the captured image matrix. However in teledermatology there are some additional issues to be taken into account, such as the transmission of the images, the display devices (screen monitors, or colour printers) and the existence of surface reflections.

In case of image-based telemedicine display devices and printers are often used but color reproduction is not problem-free; the reproduced colors may be significantly altered due to the non-standardized color management procedures of the output systems. Although cooperation between leading companies in desktop computer industry and the color reproduction industry have led to developments through the International Color Consortium (ICC), color reproduction across different systems remains a challenging task. The ICC has proposed device profiles that would ensure an open vendor-neutral, cross-platform color management. However, the common reference, the Profile Connection Space, still is not able to cover the diverse needs of the industry. The color processing is also not standardized and proprietary color definitions and gamut mappings pose significant problems [34].

At the moment the problem may often be treated through device characterization (establishment of a relationship between an original color and the signals generated). For monitors the parameters that vary and thus have to be characterized are the white and black points, chromaticity, luminance level at maximum output and “gamma” of each color channel. Methods for monitor characterization are described in [2]. For color printers the situation is more difficult since the impurities of the ink and the physical interface between ink and paper result in images full of color flaws. The color generated on paper is difficult to predict from the individual ink amounts. Empirical characterizing may be performed to associate the CMYL signals to the produced XYZ colors, using polynomial functions [16]. Unless the characterization as mentioned previously has been performed, the reproduced images are not proper for telemedical applications which require visual inspection and diagnosis.

The most serious problem for the implementation of every telemedicine system is their acceptance by the doctors. All dermatologists participated in our research expressed the opinion that illumination is decisive for the correct diagnosis. For the brighter skins the diagnosis is easier and more precise. Some expressed the opinion that also the pictures with the surface reflectances were useful for the diagnosis. The use of polarizing filters enhanced the chromatic consistency of the images, but limited the surface reflectances, thus eliminating useful image features and information about the lesion surface according to their opinion. Therefore they required at least two images for each examined skin lesion, with and without the presence of surface reflectances. The first image was used for perceiving the texture and ulceration of the lesion surface and the second for measuring the color. The ulceration of skin lesions may also be delineated by 3D stereo vision, which overcomes the limitations of 2-D imaging, provided that proper camera modeling and point matching is performed.

Other problems that were mentioned by the doctors were the inability to feel the skin as well as the refusal of certain patients to be photographed in particular body areas like the genitals. Also the inability to come in direct contact with the patient caused dissatisfaction. Obviously the implementation of a system in real time would handle this problem. Despite this, the majority of doctors that used the proposed system recognized the usefulness of teledermatology.

8. Conclusions

A new system for acquiring digital images of skin lesions has been presented. The system is able to measure objectively with high repeatability without presupposing wide experience in image assessment. The basic system features are the minimization of reflections achieved by the introduction of polarizing filters, the software-based corrections and the color constancy with regard to a reference case. The adherence to the standardized setup and measurement procedures, which have been presented, may assure the color quality and the repeatability in the images. The high image resolution is achieved through the use of digital cameras.

The system advantages can be summarized to the following:

- Acquisition of repeatable and high quality images, as regards color and resolution.
- Non-contact measurements, which prevent the local hematomas that are stimulated through pressure.
- Database for storage of the images along with the demographic patient data.
- High usability.

The system has been extended through stereo vision in order to measure lesion dimensions in 3-D providing tolerance to small spatial movements of the target. Some initial experiments have been performed with promising results. Aiming at a fully automated system we proceed to develop a dimensional representation of skin lesions and the related methods for selecting "key" points in images. Finally the medical personnel found the system features useful for image based telemedical sessions in dermatology, provided that both images, with and without of surface reflectances were transmitted for visual assessment.

References

[1] C. Balas, An Imaging Colorimeter for Noncontact Tissue Color Mapping, *IEEE Transactions on Biomedical Engineering* **444**(6) (1997), 468–474.
[2] R.S. Berns, R.J. Motta and M.E. Gorzynski, CRT colorimetry. Part I: Theory and practice, *Color Research and Applications* **18** (1993), 299–314.
[3] Vladimir Brajović and Takeo Kanade, Sensory Computing, *Critical Technologies for the Future of Computing, SPIE Proceedings* **4109** (2000), San Diego, CA.
[4] G.D. Finlayson and M.S. Drew, Constrained least-squares regression in color spaces, *Journal of Electronic Imaging* **6**(4) (1997), 484–493.
[5] C. Gonzalez Rafael and E. Richard Woods, *Digital Image Processing*, Addison-Wesley Publishing Company, 2001.
[6] A. Gutenev, V.N. Skladnev and D. Varvel, Acquisition-time image quality control in digital dermatoscopy of skin lesions, *Computerized Medical Imaging and Graphics* **25** (2001), 495–499.
[7] G. Hansen, E. Sparrow and J. Kokate et al., Wound status evaluation using color image processing, *IEEE Transactions on Medical Imaging* **16**(1) (1997), 78–86.
[8] M. Herbin, F. Bon and A. Venot et al., Assessment of healing kinetics through true color image processing, *IEEE Transactions on Medical Imaging* **12**(1) (1993), 39–43.
[9] P.C. Hung, Colorimetric calibration in electronic imaging devices using a look-up table model and interpolations, *Journal of Electronic Imaging* **2** (1993), 53–61.
[10] H.R. Kang and P.G. Andreson, Neural Network Applications to the color scanner and Printer Calibrations, *Journal of Electronic Imaging* **1** (1992), 125–134.

[11] J.E. Kaufman, ed., *IES Lighting Handbook Application Volume*, Illuminating Engineering Society of North America 1987.
[12] Kjoelen, M. Thompson, S. Umbaugh, R. Moss and W. Stoecker, Performance of Artificial Intelligence Methods In Automated Detection of Melanoma, *IEEE Engineering Medicine and Biology* **14**(4) (1995), 411–416.
[13] R.L. Lee, Colorimetric Calibration of a Video Digitizing System: Algorithm and Applications, *Color Research and Applications* **13**(3) (1988), 180–186.
[14] R.K. Lenz and R.Y. Tsai, Techniques for calibration of the scale factor and image center for high accuracy 3-D machine vision metrology, *IEEE Transactions on Pattern Analysis and Machine Intelligence* **10**(5) (1988), 713–720.
[15] M. Loane, H. Gore, R. Corbet and K. Steele, Effect of Camera performance on diagnostic accuracy, *Journal of Telemedicine and Telecare* **3** (1997), 83–88.
[16] L.W. MacDonald, Developments in color management systems, *Displays* **16**(4) (1996), 203–211.
[17] I. Maglogiannis, Automated Segmentation and Registration of Dermatological Images, *The 2002 International Conference on Parallel and Distributed Processing Techniques and Applications*, Las Vegas, Nevada, USA, 2002, pp. 121–126.
[18] I. Maglogiannis, C. Caroni, S. Pavlopoulos and V. Karioti, *Utilizing Artificial Intelligence for the Characterization of Dermatological Images*, 4th International Conference Neural Networks and Expert Systems in Medicine and Healthcare, Milos Island, Greece, 2001, pp. 362–368.
[19] S.O. Mason and A. Gruen, Automatic Sensor placement for accurate dimensional inspection, *Computer Vision and Image Understanding* **61**(3) (1995), 454–467.
[20] M. Nishik and C. Foster, Analysis of Skin Erythema Using True Color Images, *IEEE Transactions on Medical Imaging* **16**(6) (1997), 711–716.
[21] M. Osawa and S. Niva, A portable diffuse reflectance spectrophotometer for rapid and automatic measurement of tissue, *Measurements Science Technology* **4** (1993), 668–676.
[22] J. Salvi, X. Armangue and J. Battle, A comparative review of camera calibrating methods with accuracy evaluation, *Pattern Recognition* **35** (2002), 1617–1635.
[23] E. Trucco and A. Verri, *Introductory Techniques for 3-D Computer Vision*, Prentice Hall, Upper Saddle River, NJ, 1998.
[24] R.Y. Tsai, A versatile camera calibration technique for high accuracy 3-D machine vision metrology using off the shelf TV cameras and lenses, *IEEE Journal of Robotics and Automation* **3**(4) (1987), 323–344.
[25] S.E. Umbaugh, R.H. Moss and W.V. Stoecker, Automatic Color Segmentation of Images with application to detection of Variegated Coloring in Skin Tumors, *IEEE Engineering in Medicine and Biology* **8**(4) (1989), 43–52.
[26] S.E. Umbaugh, Y. Wei and M. Zuke, Feature Extraction in Image Analysis, *IEEE Engineering in Medicine and Biology* **16**(4) (1997), 62–73.
[27] J. Young and L. Gerbrands, Vliet, *Fundamentals of Image Processing*, Delft University of Technology, Netherlands, 1998.
[28] J. Sanders, B. Goldstein, D. Leotta and K. Richards, Image proccesing tecniques for quantitative analysis of skin structures, *Computer Methods and Programs in Biomedicine* **59** (1999), 167–180.
[29] Goldon, Gary and Nuckols, *Interior lighting for designers*, Third ed., John Willey and Sons, 1995.
[30] D.L. Ramsey and A.B. Fox, The ability of primary care physicians to recognize the common dermatoses, *Arch. Dermatol.* **117** (1981), 620–622.
[31] R.J. Pariser and D.M. Pariser, Primary care physicians errors in handling cutaneous disorders, *J Am Acad Dermatol* **17** (1987), 239–245.
[32] H.J. Trussell, Application of Set Theoretic Methods to Color Systems, *Color Research and Applications* **16**(1) (1991), 31–41.
[33] GretagMacbeth Corporation http://www.gretagmacbeth.com.
[34] International Color Consortium http://www.color.org.
[35] Kodak Corporation, CMOS vs CCD and the future of imaging, www.kodak.com/US/en/corp/researchDevelopment/technologyFeatures/cmos.shtml.